Biochimica et Biophysica Acta 1827 (2013) 738–744

Contents lists available at SciVerse ScienceDirect

Biochimica et Biophysica Acta

journal homepage: www.elsevier.com/locate/bbabio

An NMR comparison of the light-harvesting complex II (LHCII) in active and photoprotective states reveals subtle changes in the chlorophyll *a* ground-state electronic structures

Anjali Pandit [a,*], Michael Reus [b], Tomas Morosinotto [c], Roberto Bassi [d], Alfred R. Holzwarth [b], Huub J.M. de Groot [e]

[a] Faculty of Sciences, Dept. of Physics and Astronomy, VU University Amsterdam, De Boelelaan 1081 HV Amsterdam, The Netherlands
[b] Max-Planck-Institute for Chemical Energy Conversion (MPI-CEC), [1] Stiftstrasse 34–36, D-45470 Mülheim an der Ruhr, Germany
[c] Department of Biology, University of PadovaVia Ugo Bassi 58 B, 35121 Padova, Italy
[d] Laboratory of Photosynthesis, Department of Biotechnology, University of Verona, Strada Le Grazie 15 Verona, 37134, Italy
[e] Leiden Institute of Chemistry, Leiden University, P.O. Box 9502, 2300 RA Leiden, The Netherlands

ARTICLE INFO

Article history:
Received 18 December 2012
Received in revised form 14 February 2013
Accepted 23 February 2013
Available online 4 March 2013

Keywords:
Non-photochemical quenching
Photosynthetic light-harvesting
Major light-harvesting complex II
Conformational switch

ABSTRACT

To protect the photosynthetic apparatus against photo-damage in high sunlight, the photosynthetic antenna of oxygenic organisms can switch from a light-harvesting to a photoprotective mode through the process of non-photochemical quenching (NPQ). There is growing evidence that light-harvesting proteins of photosystem II participate in photoprotection by a built-in capacity to switch their conformation between light-harvesting and energy-dissipating states. Here we applied high-resolution Magic-Angle Spinning Nuclear Magnetic Resonance on uniformly ^{13}C-enriched major light-harvesting complex II (LHCII) of *Chlamydomonas reinhardtii* in active or quenched states. Our results reveal that the switch into a dissipative state is accompanied by subtle changes in the chlorophyll (Chl) *a* ground-state electronic structures that affect their NMR responses, particularly for the macrocycle ^{13}C4, ^{13}C5 and ^{13}C6 carbon atoms. Inspection of the LHCII X-ray structures shows that of the Chl molecules in the terminal emitter domain, where excited-state energy accumulates prior to further transfer or dissipation, the C4, 5 and 6 atoms are in closest proximity to lutein; supporting quenching mechanisms that involve altered Chl–lutein interactions in the dissipative state. In addition the observed changes could represent altered interactions between Chl*a* and neoxanthin, which alters its configuration under NPQ conditions. The Chls appear to have increased dynamics in unquenched, detergent-solubilized LHCII. Our work demonstrates that solid-state Nuclear Magnetic Resonance is applicable to investigate high-resolution structural details of light-harvesting proteins in varied functional conditions, and represents a valuable tool to address their molecular plasticity associated with photoprotection.

1. Introduction

Light is the source of energy for photosynthetic organisms but, when in excess, it also drives the formation of reactive oxygen species and consequently photo-inhibition. Photosynthetic organisms evolved mechanisms to regulate light-harvesting efficiency in response to variable light intensity as for avoiding oxidative damage. Non-photochemical quenching (NPQ) consists in the rapid dissipation of excitation energy as heat and is manifested in photosynthetic light-harvesting antennae of oxygenic photosynthetic organisms. These antennae have a dual role: they are designed for optimal light-harvesting, and when exposed to excess light they can switch into a light-energy dissipating state. In higher plants and most algae the major component of rapid fluorescence quenching is the pH- or energy-dependent component, qE. In plants, the qE energy dissipation process is cooperatively induced by a decrease in lumen pH, via protonation of PsbS proteins, and by the activation of zeaxanthin synthesis via a xanthophyll cycle [1,2]. Upon qE activation, antenna complexes undergo a conformational change generating quenching sites. In algae, PsbS is absent [3] while the sensor of lumenal pH triggering of NPQ is the LhcSR protein [4], a pigment-binding complex with a short fluorescence lifetime [5]. In algae as well other organisms, antenna complexes participate in quenching and specific involvement has been evidenced for Lhcbm1, the major component of the major light-harvesting complex II (LHCII) [6,7]. This result is consistent with the Lhcbm1 component of *Chlamydomonas* LHCII undergoing a conformational change contributing to the quenching reaction synergic with quenching in LhcSR. This effect would be similar to that described for PsbS on Lhcb proteins [8].

* Corresponding author. Tel.: +31 20 5987937; fax: +31 20 5987899.
E-mail address: a.pandit@vu.nl (A. Pandit).
[1] Previous known as Max-Planck-Institute for Bioinorganic Chemistry.

0005-2728/$ – see front matter
http://dx.doi.org/10.1016/j.bbabio.2013.02.015

Several models have been proposed for the mechanisms of de-excitation of the chlorophyll (Chl) first excited state under NPQ conditions, involving a change in pigment configurations in the light-harvesting antennae of photosystem II. Proposed quenching mechanisms for plants include formation of carotenoid (Car) radical cations in the minor antennae that quench the Chl excited-state by Chl–zeaxanthin charge transfer [9], Chl–Chl charge-transfer states characterized by far red fluorescence emission [10], excitation energy transfer from Chl to a low-lying Car excited state occurring the major antenna [11–13] and low excitonic Car–Chl states [14]. The different proposed mechanisms are not exclusive and may operate in parallel. Reduced Chl excited-state lifetimes can be reproduced *in-vitro* in self-aggregated antenna proteins and comparison of their spectroscopic properties suggests that the *in vitro* and *in vivo* photophysical quenching mechanisms are similar [10,12,15]. LHCII complexes immobilized in a gel, which are prevented from aggregation, switch into a fluorescence-quenched state upon detergent depletion [16] and single antenna proteins fluctuate between fluorescent and quenched states modulated by the physic-chemical environment [17], supporting a quenching model that includes intra-molecular conformational changes. Two high-resolution X-ray structures are available of pea [18] and spinach [19] LHCII trimers but to which extent they represent the energy-dissipating or light-harvesting state is controversial [13,20] and LHCII may adopt a particular structure in each crystal type [21]. Single LHCII trimer complexes reconstituted in lipid nanodiscs retain their light-harvesting state, but show small spectral changes compared to unquenched LHCII trimers in detergent micelles, demonstrating that LHCII exhibits conformational variability within its light-harvesting state [22].

In this work, we present high-resolution MAS-NMR data of LHCII complexes prepared in light-harvesting and light-energy dissipating states. Photosynthetic light-harvesting proteins represent a challenge for NMR since they are oligomers that are densely packed with chromophores, which in the case of LHCII correspond with ~one third of the total molecular weight of the complex [23]. In addition, the low yields that are generally obtained from recombinant reconstituted light-harvesting complexes are insufficient for large-scale preparations, and isotope labeling of photosynthetic organisms is required for the preparation of NMR samples. In earlier work this was achieved for *Rhodopseudomonas acidophila* purple-bacteria, which permitted us to selectively compare the bacteriochlorophyll (BChl) ground-state electronic structures of the different BChls in intact peripheral and core light-harvesting oligomers [24]. NMR protein secondary shifts revealed subtle strain in the protein backbone fold, induced by the dense pigment–protein packing in the complexes [25], an effect that was not resolved in the X-ray structures. We have recently shown that uniformly ^{13}C-labeled LHCII can be obtained in large quantities from *Chlamydomonas reinhardtii* green algae grown on ^{13}C-acetate-labeled media [26]. The LHCII complex of *C. reinhardtii* is homologue to LHCII of plants (see Figure S1 in the Supporting Information section for a sequence comparison of Lhcbm1 and Lhcb1). Here, we use the NMR spectra of *C. reinhardtii* LHCII together with the available X-ray structures of higher-plant LHCII to assign a large number of NMR correlation signals to pigment and protein nuclear-spin clusters. Subsequently, ^{13}C–^{13}C dipolar correlation NMR spectra of LHCII complexes are analyzed in detail to provide a structural comparison of LHCII in its light-harvesting and energy-dissipating states.

2. Materials and methods

2.1. Sample preparation

Uniformly labeled ^{13}C-LHCII was prepared as described in Ref. [26]. The LHCII proteins were isolated from thylakoid membranes by sucrose gradient using 0.6% α-dodecyl-maltoside (α-DM), as shown in Figure S1 in the Supporting Information section. To obtain highly quenched LHCII aggregates, the LHCII complexes in β-DM buffer were incubated with BioBeads for extraction of β-DM, after which the sample was concentrated with 30kD filters. The LHCII aggregates were obtained from the sediments on the filters and directly loaded into a 4 mm cramps rotor. For NMR samples of LHCII in a fluorescent, light-harvesting state, the detergent-solubilized LHCII was concentrated to a final concentration of about 100 mg/ml taking pigments and protein together. Fluorescence experiments performed to reveal the functional states of the LHCII preparations are described in the Supporting Information section.

2.2. Solid-state NMR

2D ^{13}C–^{13}C proton driven spin diffusion NMR experiments (PDSD) were collected with a Bruker AV750 17.4 T (^{1}H frequency 750 MHz) solid state NMR spectrometer equipped with a triple MAS resonance probe. The LHCII samples contained ~15 mg of protein loaded in a 4 mm CRAMPS rotor and were stepwise cooled to temperatures of 223–243 K during slow spinning. Spectra were collected with various mixing times varying from 10 to 300 ms and using rotor frequencies of 13000 or 11500 kHz. The ^{13}COOH resonance of U–[^{13}C, ^{15}N]–tyrosine/HCl was used as an external chemical shift reference and all chemical shifts are referenced to tetramethylsilane (TMS). The proton 90° pulse was set to 3.1 μs. ^{13}C B_1 field strengths of ~50 kHz corresponding with a cross polarization time of 2.0 ms were applied during a ramped CP sequence. Two-pulse phase modulation (TPPM) decoupling was applied during the t_1 and t_2 periods. The specific processing parameters of the presented spectra are provided in the Supporting Information section.

2.3. Structure modeling and chemical shift prediction

Based on the LHCII crystal structure of pea (*Pisum sativum*, PDB ID: 2BHW) a homology structure of *C. reinhardtii* LHCII was build based on the Lhcbm1 sequence of *Chlamydomonas* LHCII using the SWISS-MODEL Expasy web server [27–31]. The backbone C_α, C_β and CO and the C_γ and C_δ protein chemical shifts of the homology structure were predicted using the program SHIFTX2 [32]. Predicted correlations from ^{13}C–^{13}C NMR homonuclear correlation spectroscopy were obtained using the FANDAS program [33] available at http://www.wenmr.eu/services/FANDAS/html/main.php.

3. Results and discussion

3.1. The fluorescence states of detergent-solubilized (**U**) and aggregated (**Q**) LHCII

LHCII trimer complexes were prepared in their active light-harvesting, i.e. fluorescent state (sample **U**) and in energy-dissipating, strongly fluorescence-quenched and aggregated state (sample **Q**). Quenching of Chl singlet excited-state energy by NPQ is quantified by the parameter $K_d = F_m/F'_m - 1$, which reflects the reduction in Chl fluorescence F'_m compared to the unquenched state F_m. Sample **Q** contained detergent-depleted, self-aggregated LHCII complexes with $K_d = 19$. This sample exists in strongly quenched and strongly aggregated conformations based on its spectral signatures at 77 K, i.e. the appearance of a second fluorescence band around 700 nm, as shown in Figure S3 in the SI section. Sample **U**, representing LHCII in its light-harvesting state, was prepared in β-DM detergent buffer solution above the critical micelle concentration (CMC) and concentrated to ~100 mg/ml for the NMR experiments. Time-resolved fluorescence experiments were performed on the concentrated LHCII-β-DM micelle solution to verify that the complexes retained their fluorescent state at high concentration. The decay-associated fluorescence spectra of **U** are shown in Figure S2 and the fluorescence lifetimes are presented in Table S1, SI section. Sample **U** has $K_d = 1.2$ and an average

fluorescence lifetime $<\tau_f> = 1.7$ ns, which is reduced compared to the 3.8 ns lifetime found for diluted solutions of LHCII trimers in 0.03% β-DM, but significantly longer than lifetimes that are observed for LHCII crystals (0.3–1 ns) [20] or for LHCII aggregates [34] (<0.3 ns). The major fluorescence component of **U** decays with 2.5 ns (SI, Table S1), which is similar to the fluorescence lifetimes found for Chl in thylakoid membranes *in vivo* under light-harvesting conditions [35] and for membrane-reconstituted LHCII *in vitro* at low protein/lipid densities [36]. For these systems, weak protein–protein interactions in the membrane are thought to cause small reduction of the fluorescence lifetime compared to isolated LHCII trimers and such interactions may also occur in very crowded protein-micelle solutions.

3.2. Protein ^{13}C NMR responses in the aliphatic and carbonyl region

To compare the global protein folds of LHCII in **Q** and **U**, in Fig. 1 the ^{13}C–^{13}C NMR spectra of **Q** (red) and **U** (blue), collected with the same mixing time, are overlaid in the aliphatic and carbonyl region. A homology structure for *C. reinhardtii* LHCII based on plant LHCII was constructed for prediction of the protein NMR ^{13}C chemical shifts, from which a simulated ^{13}C–^{13}C NMR correlation plot was generated (Fig. 1, black dots). While **Q** shows a more intense 2D CP/MAS correlation response for several side chain spin clusters with additional and stronger correlation signals compared to **U**, the overlay of the spectra shows that both **Q** and **U** give rise to highly resolved correlation data sets with very similar chemical shift patterns and backbone correlation signals. This shows that the global fold is preserved going from detergent-solubilized to strongly aggregated LHCII. The predicted NMR correlation plot is well in line with the experimental data, showing that the experimental NMR spectra are in agreement with the *C. reinhardtii* LHCII homology structure. In the experimental spectra, correlation signals of the lipids and the Chl aliphatic groups are visible while they are not included in the predicted correlations. In fact, a large number of cross signals detected in the region 70–80 ppm for **Q** are attributable to the sugar moieties of the lipid head groups of protein-associated lipids that remain attached upon LHCII isolation. The correlation signals for the various amino-acid types separate into clusters and are identified aided by the predicted correlation spectrum for alanine (A), threonine (T), valine (V), proline (P), serine (S), leucine (L) and isoleucine (I) in the aliphatic region and for glycine (G), alanine (A) and the side chain carboxyls of glutamic acid (E) and aspartic acid (D) in the COO region.

3.3. Chl NMR signals in the aromatic region

Fig. 2 shows representative ^{13}C–^{13}C spectra of **Q** in which the LHCII Chl signals are well-resolved. Spectra of similar quality in the Chl region were obtained from **U**. The xanthophyll response is dispersed over a narrow region between ~132 and 140 ppm, as shown in Figure S4 in the SI section. Based on ^{13}C chemical shift assignments of Chl*a* and *b* in Ref. [37], Chl NMR cross-correlation signals are resolved for the carbon macrocycle atoms. The Chl C5-4/6 cross correlations (corresponding atoms drawn in purple in the Chl chemical structure) for Chl*b* and Chl*a* are set apart, owing to the fact that for Chl*b*, the C4 and C6 signals overlap while for Chl*a* they are several ppm separated, and since the C5 signals of Chl*b* are ~3 ppm shifted downfield compared to Chl*a*. The Chl C10-9/11 correlation signals (corresponding atoms drawn in red in the Chl chemical structure) can also be classified for Chl*b* and Chl*a* since for Chl*b*, the C9 and C11 chemical shifts are ~6 ppm separated, while for Chl*a* the separation is only ~1.5 ppm. The C10-9/11 cross peaks for Chl*b* show a remarkable dispersion for different Chls, and the chemical shifts for the Chl*b* C10 ring atoms are distributed over a range from 110 to 115 ppm. Five out of the six Chl*b* can form hydrogen bonds to the 7-formyl groups according to the LHCII X-ray structures [18,19]. The variation of the Chl*b* C9-10-11 chemical shifts can be due to structural displacements

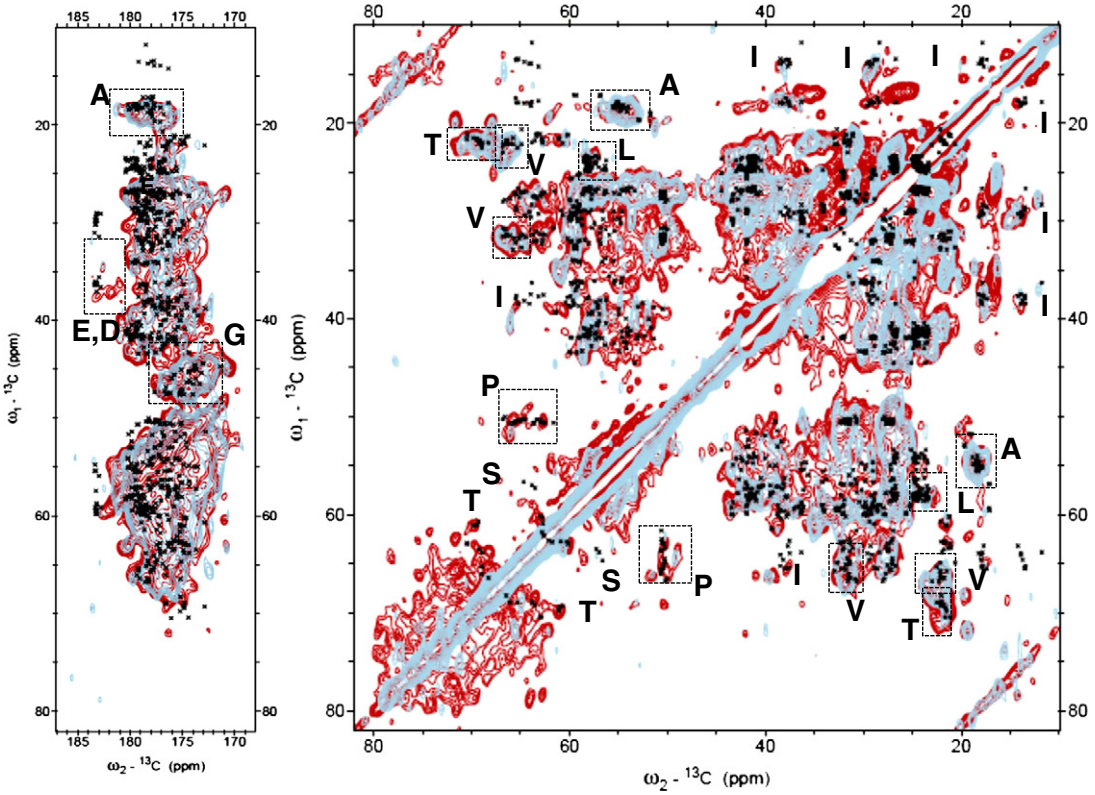

Fig. 1. ^{13}C–^{13}C NMR homonuclear correlation spectra in the aliphatic and COO region of *C. reinhardtii* LHCII aggregates, sample **Q** (red), detergent-solubilized LHCII, sample **U** (light blue), and structure-predicted protein correlations (black crosses). The predicted correlation plot was generated from a *C. reinhardtii* LHCII homology structure.

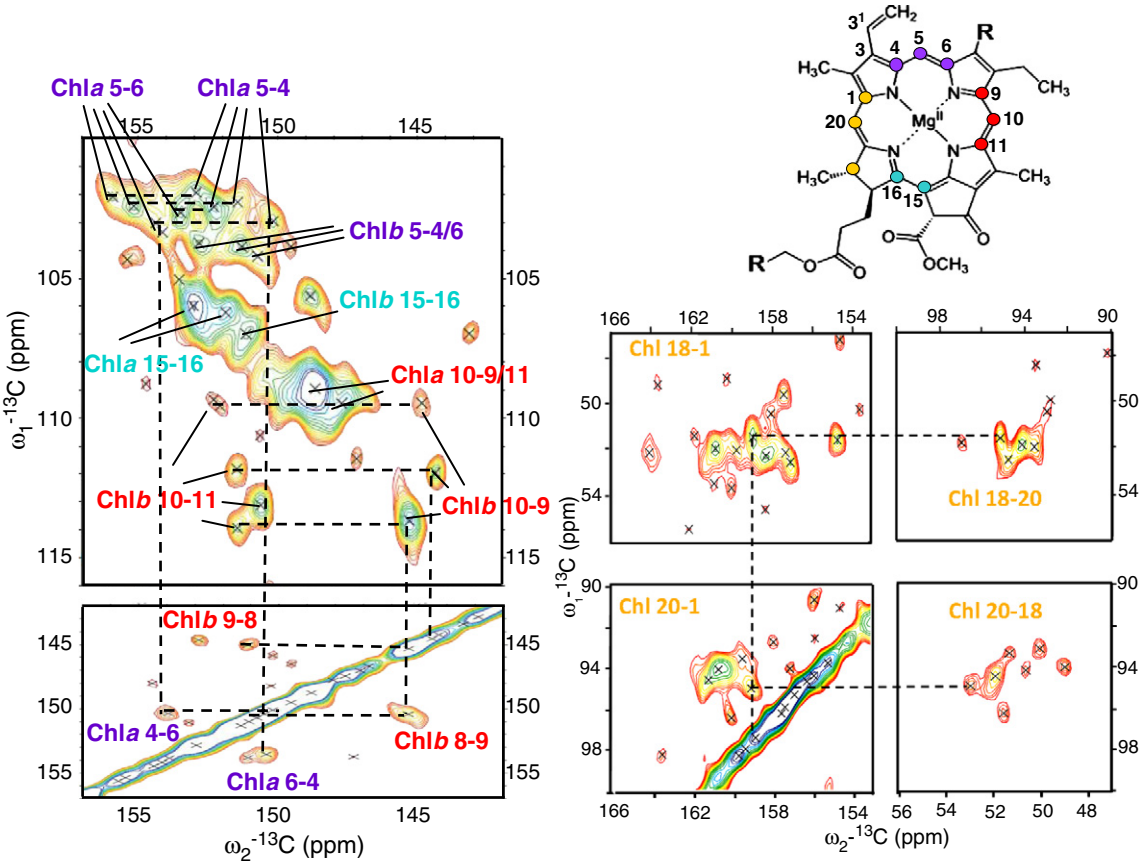

Fig. 2. Chl NMR responses resolved in ^{13}C–^{13}C NMR homonuclear correlation spectra of **Q**. Color codes of the assignments in the NMR spectra match with the corresponding atoms in the Chl chemical structure.

of the Chl macrocycles when hydrogen bonds are formed to the 7-formyl side chains, since chlorin macrocycle chemical shifts are very sensitive to structural deformation [24]. The overall dispersion of the chemical shifts within the Chl nuclear spin clusters, which is also observed in spectra of **U**, confirms static disorder of the various Chl molecules in LHCII that reside in heterogeneous protein environments. The different site energies for individual Chls due to static disorder are responsible for the inhomogeneous broadening observed in optical spectra and are essential for fast and directional light-energy transfer towards the photosynthetic reaction center *in vivo* [38].

3.4. A structural comparison of LHCII in light-harvesting and energy-dissipating states

Because the Chl responses in the aromatic region are less congested than the carotenoid responses and the aliphatic and carbonyl protein responses, we focus on this part of the spectrum for a detailed comparison between **U** and **Q**. Fig. 3 presents an overlay of ^{13}C–^{13}C correlation data for **U** (blue) and **Q** (red) that were obtained at 224 K with same spectrometer settings and processed in the same way. Both data sets are plotted with the threshold intensity set at 8 times the noise level. Significant Chl*a* peak shifts are observed for C5-4/6 cross correlations, indicated by arrows in the spectrum. The weaker Chl*b* C5-4/6 correlations fall below the threshold intensity at these settings. The Chl*a* peak shifts show that conformational changes occur between **U** and **Q** that alter the structure or local environment of Chl*a* around the 5 methine carbon, which represents a flexing point of the ring. The widths of the shifted cross peaks are around 2 ppm for **U** and between 2 and 3 ppm for **Q** which suggest that they represent the averaged signals of several Chl molecules. To improve the spectral resolution, NMR spin diffusion experiments of **U** and **Q** were optimized individually for visibility of the Chl C4, C5 and C6 signals by adjusting the spin-diffusion mixing times and temperature, and resulting spectra are presented in Fig. 4 (left, in blue: spectrum of **U** and right, in red:

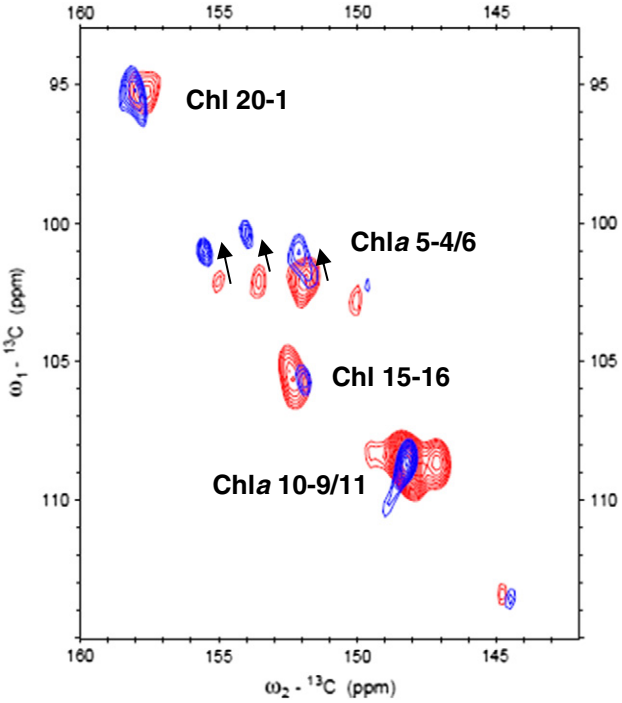

Fig. 3. Comparison of the Chl NMR responses of **Q** (red) and **U** (blue) in the aromatic region. Significant shifts between cross peaks in spectra of **U** and **Q** are indicated by the black arrows.

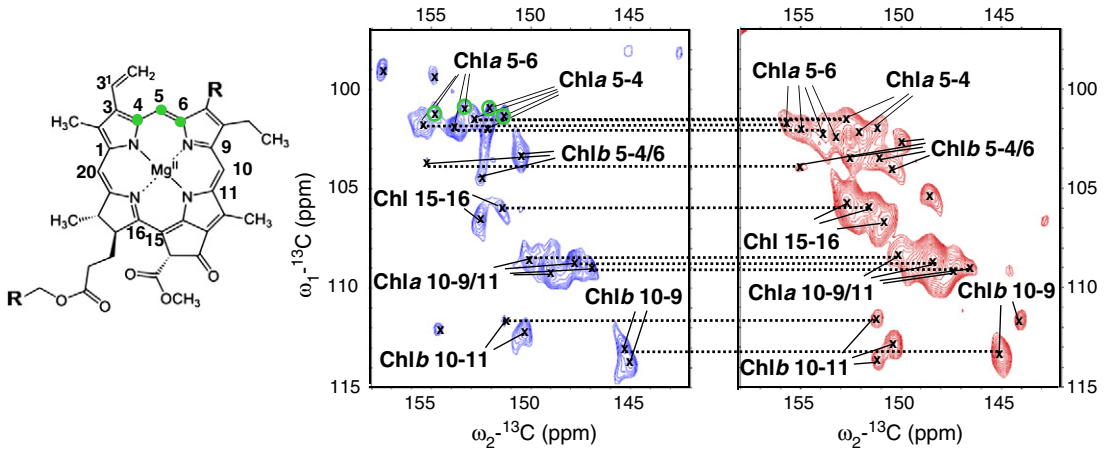

Fig. 4. ^{13}C–^{13}C correlation spectra of **Q** (red, right spectrum) and **U** (blue, left spectrum) optimized for the Chl C5-4/6 cross signals. Cross peaks that are conserved between **U** and **Q** are indicated by the connecting lines. Shifted Chl C4, 5, 6 NMR responses in **U** is indicated by the green circles. The C4, C5 and C6 ring atoms are highlighted in the Chl chemical structure.

spectrum of **Q**). In the spectra in Fig. 4, several narrowly-spaced Chl peaks are resolved for the C5-4/6 cross correlations. Two sets of C5-4 and C5-6 correlation peaks appear shifted in the spectra of **U**, indicated by the green circles and suggesting that at least two Chls have altered NMR responses, and the overall chemical shift pattern of the C4, 5 and 6 Chl carbon signals appears changed. Compared to the spectrum of **Q**, in the spectrum of **U** in Fig. 4 less Chl C15-16 and Chl*b* C5-4/6 correlations are observed, which could be due to the longer mixing time that was used. From the data sets cannot be excluded that also for these Chls carbon atoms chemical shifts differences occur between **U** and **Q**.

The molecular mechanism(s) of NPQ are proposed to involve subtle conformational changes in the local environment of the quencher pigments [12]. It has been demonstrated that structural changes in the order of an Ångstrom as well as changes in polarity are sufficient to alter the spectroscopic features of natural and artificial light-harvesting systems [39–41]. Such changes are expected to have a pronounced effect on the NMR chemical shifts of the involved pigments. The ground-state electronic structures of protein-bound chromophores are defined by the energetic potential of the protein matrix and are sensitive to electric-field effects originating from charged groups in the vicinity, hydrogen-bonding and van der Waals packing interactions. The observation here of Chl*a* NMR peak shifts prominently at the site of C4, C5 and C6 macrocycle ring carbons may provide a key to structural changes associated with NPQ. Below, possible origins of the Chl*a* peak shifts are discussed in the frame of existing knowledge on the structure and functioning of LHCII.

Upon light excitation, fast energy transfer takes place among the pigments toward the terminal Chl*a* fluorescence-emitting domain formed by the Chl610/611/612 cluster [38], where excited-state energy accumulates prior to further transfer or dissipation. According to several quenching models based on Chl–Lut energy transfer or low excitonic states, Lut620 interacts with Chl*a* within the terminal emitting domain [12,42,43] and the fluorescence switch involves a change in distance or orientation that brings Chl*a* and Lut620 in closer contact [12]. In the LHCII crystal structures, it is striking that the shortest Chl–Lut620 distances are between the Lut620 polyene chain and the C4-5-6 atoms of Chl610 and 612 of which the latter Chl is in coplanar contact with Lut620 [18]. This is shown in Fig. 5A, where the structures of Lut620, Chl610 and 612 are taken from the LHCII crystal structure of pea (*P. sativum*, PDB ID: 2BHW) and the Chl C4-5-6 atoms are highlighted in green. The observed NMR peak shifts could be explained by altered interactions between Lut620 and Chl610 and 612 in the dissipative state that for instance cause structural deformation of the Chl rings. An analysis of out-of-plane Chl macrocycle distortions in the LHCII structure shows macrocycle displacements for Chl612 near ring I and II, where the C4, C5 and C6 ring carbons are located [44]. The NMR chemical shifts of the macrocycle 5-methine ring atoms are very sensitive to ring structural displacements, and small changes in the Chl conformational structure due to altered Chl–lutein interactions would affect the chemical shifts of the involved atoms [24].

In addition, the two LHCII crystal structures show differences for the orientation of a methionine (Met) group close to Chl610, which suggests conformational flexibility of this group that affects the Chl610

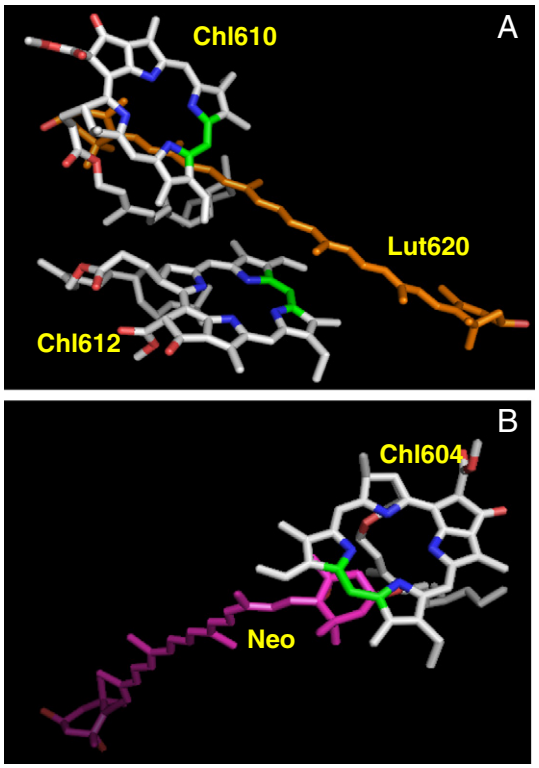

Fig. 5. Chl–carotenoid interactions in the LHCII crystal structure of pea (*Pisum sativum*, PDB ID: 2BHW) [18]. A; Chl610, Chl612 and Lut620, B; Neo and Chl604. The Chl*a* C4, 5 and 6 ring carbon atoms are highlighted in green and are in close proximity to the carotenoids (inter-distances ≤4 Å).

site energy according to Muh et al. [45]. Since the Met side chain is close to the C4-5-6 ring atoms of Chl610, conformational changes of this group will affect the Chl610 C4-5-6 NMR chemical shifts.

The third Chl*a* in the terminal emitter domain, Chl611, is ligated by the phosphodiester group of a phosphatidyl glycerol (PG) lipid molecule. The same work of Muh et al. demonstrated that the site energy of this pigment is dominated by the presence of the negatively-charge head group of PG on one side and the positively-charged lysine Lys182 on the other side. The lipid oxygen atoms are oriented toward the Chl611 C4-5-6 atoms, and the Chl611 C4-5-6 chemical shifts should be sensitive to small changes in the orientation of the PG head group.

While the neoxanthin (Neo) carotenoid is not directly involved in the quenching process, the formation of NPQ *in vivo* and quenching of LHCII *in vitro* is associated with a twist in the Neo conformation [12,46]. Short pigment–pigment distances involving Chl*a* C4-5-6 atoms exist for Chl*a* 604 and the head group of Neo, as shown in Fig. 5B. The site energy of Chl604 is dominated by the presence of a tyrosine hydroxy (Tyr112) [45]. The observed NMR peak shifts therefore could also include changes in the local environment of Chl604 in the quenched state caused by a re-orientation of Neo and modified interactions with Tyr112.

In addition to specific pigment or protein interactions, the chemical shifts of Chls in the protein exterior, including the terminal-domain pigments Chl611 and 612, will be sensitive to polarity changes of the protein micro-environment. This micro-environment is different for LHCII trimers embedded in detergent micelles than for LHCII aggregates, which could lead to shifted NMR responses for the exposed Chl sites. To distinguish between possible origins of the observed NMR peak shifts, the magnitudes of the effects on the Chl chemical-shifts of specific electrostatic and structural interactions in LHCII as discussed here will have to be further tested by theoretical calculations.

3.5. Dynamics of LHCII in light-harvesting and energy-dissipating states

Comparing ^{13}C–^{13}C NMR spectra of **Q** and **U** collected at 244 K, the Chl signals are weaker in the spectra of **U**, in particular those of the Chl C4-5-6 ring atoms. This is illustrated in Fig. 6, which shows an overlay of spectra from **U** and **Q** collected at 244 K in the region of the Chl aromatic carbons. The spectra were collected with same spectrometer settings and processed in the same way, and are plotted with the threshold intensity set at 7 times the noise level. With this threshold setting, the Chl C5-4/6 correlations are not visible in the spectrum of **U**, while in the spectrum of **Q** both Chl*a* and Chl*b* C5-4/6 correlation signals are present. The differences in sensitivity suggests that the Chls in LHCII have enhanced flexibility in **U**, i.e. increased motions on the micro- to millisecond timescale, resulting in smaller dipolar couplings that attenuate polarization transfer. The protein NMR responses in Fig. 1 are also acquired from data sets obtained at 244 K, and these show fewer correlations for **U** compared to **Q** in the aliphatic region, indicative of increased flexibility of the protein side chains in **U** as well. Chl cross peaks start to emerge in spectra of **U** when the temperature is set below 230 K. Below this temperature also signals of the lipid head groups emerge in the spectra of **U**. Apparently, around 230 K the protein-attached lipids become immobilized by freezing out of the motions of the solvent molecules and of protein-attached water and detergent shell molecules. In contrast, lipid signals emerge in spectra of **Q** already at elevated temperatures (Fig. 1, in the red spectrum of **Q** at 244 K the lipid head group signals appear between 70 and 90 ppm). This contrast can be explained by the low water content and condensed packing of the LHCII complexes in aggregates that probably provide a larger hydrophobic scaffold for the proteins than the detergent micelles surrounding the individual LHCII trimers in **U**. In similar way, the low-water content and condensed packing of LHCII inside aggregates could cause differences in Chl dynamics between **U** and **Q** of pigments located in the peripheral regions of the complex.

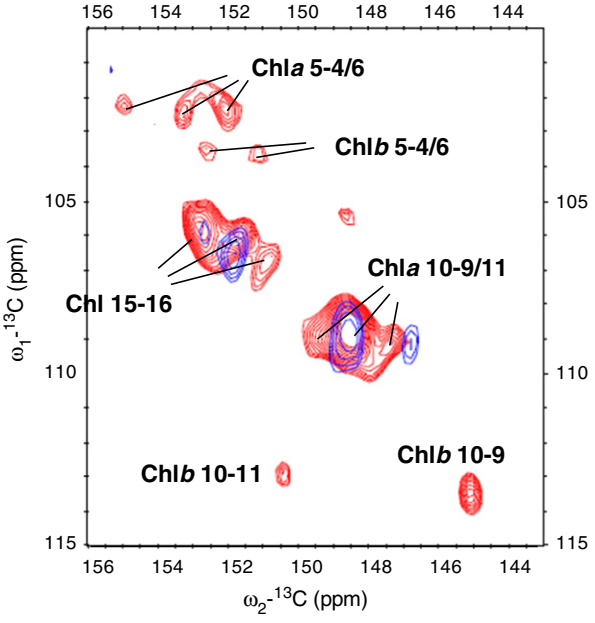

Fig. 6. NMR responses of the Chl aromatic carbons in spectra of **Q** (red) and **U** (blue) obtained at 244 K, illustrating that cross peak intensities in the spectrum of unquenched LHCII (**U**) are reduced above the glass transition temperature due to increased Chl dynamics.

The possibility of LHCII internal conformational changes was disputed based on the rigidity of the LHCII pigment–protein complex that is expressed by the low B-factors of the LHCII crystal structures [47]. However, according to our NMR data, in unquenched LHCII trimers in detergent micelles, i.e. conditions that might be more close to the native light-harvesting state of the protein, the Chls exhibit restricted dynamics that is reduced in the aggregated, quenched state. This implies that the transition into a dissipative state involves conformational or environmental changes at specific Chl sites, which is indeed observed for Chl*a*. We propose that the reduced mobility of Chls in LHCII aggregates, or similarly in LHCII crystals, has a role in promoting the quenched state. Inhibition of specific dynamic motions will moderate the pigment and protein conformational energy landscape, which then could shift the thermodynamic equilibrium between different conformations towards the energy-dissipating states.

4. Conclusions

By uniform ^{13}C isotope enrichment in combination with solid-state NMR spectroscopy, protein and pigment high-resolution structural details of oxygenic light-harvesting complexes in light-harvesting and energy-dissipative states were compared. The results reveal that the transition of LHCII into an energy-dissipative state *in vitro* is accompanied by subtle changes in the ground-state electronic structure of Chl*a* particularly at the sites of C4, C5 and C6 macrocycle carbon atoms. Based on present knowledge of the LHCII structure and function, we suggest that these changes involve the Chls in the terminal-emitter domain (Chl610, 611 and 612) that are close to Lut, supporting quenching mechanisms that involve altered Chl–Lut interactions in the dissipative state. In addition, the observed NMR changes could involve Chl604 that is near the Neo head group. The results presented here can be considered a starting point to evaluate conformational changes associated with the photophysical process of NPQ, now that it has been shown that the structural flexibility of photosynthetic light-harvesting complexes can be probed by MAS NMR at great detail under non-crystallized and controlled, varying functional conditions.

Acknowledgement

This work was supported by HARVEST Marie Curie Research Training Network (PITN-GA-2009-238017). Dr. Karthick Babu Sai Sankar Gupta, Fons Lefeber and Kees Erkelens (Leiden, The Netherlands) are gratefully acknowledged for their help with the solid-state NMR spectroscopy.

Appendix A. Supplementary data

Supplementary data to this article can be found online at http://dx.doi.org/10.1016/j.bbabio.2013.02.015.

References

[1] P. Horton, A.V. Ruban, M. Wentworth, Allosteric regulation of the light-harvesting system of photosystem II, Philos. Trans. R. Soc. Lond. B Biol. Sci. 355 (2000) 1361–1370.
[2] I. Szabo, E. Bergantino, G.M. Giacometti, Light and oxygenic photosynthesis: energy dissipation as a protection mechanism against photo-oxidation, EMBO Rep. 6 (2005) 629–634.
[3] G. Bonente, F. Passarini, S. Cazzaniga, C. Mancone, M.C. Buia, M. Tripodi, R. Bassi, S. Caffarri, The occurrence of the psbS gene product in *Chlamydomonas reinhardtii* and in other photosynthetic organisms and its correlation with energy quenching, Photochem. Photobiol. 84 (2008) 1359–1370.
[4] G. Peers, T.B. Truong, E. Ostendorf, A. Busch, D. Elrad, A.R. Grossman, M. Hippler, K.K. Niyogi, An ancient light-harvesting protein is critical for the regulation of algal photosynthesis, Nature 462 (2009) 518–522.
[5] G. Bonente, M. Ballottari, T.B. Truong, T. Morosinotto, T.K. Ahn, G.R. Fleming, K.K. Niyogi, R. Bassi, Analysis of LhcSR3, a protein essential for feedback de-excitation in the green alga *Chlamydomonas reinhardtii*, PLoS Biol. 9 (2012) 17.
[6] D. Elrad, K.K. Niyogi, A.R. Grossman, A major light-harvesting polypeptide of photosystem II functions in thermal dissipation, Plant Cell 14 (2002) 1801–1816.
[7] P. Ferrante, M. Ballottari, G. Bonente, G. Giuliano, R. Bassi, LHCBM1 and LHCBM2/7 polypeptides, components of major LHCII complex, have distinct functional roles in photosynthetic antenna system of *Chlamydomonas reinhardtii*, J. Biol. Chem. 287 (2012) 16276–16288.
[8] S. de Bianchi, M. Ballottari, L. Dall'Osto, R. Bassi, Regulation of plant light harvesting by thermal dissipation of excess energy, Biochem. Soc. Trans. 38 (2010) 651–660.
[9] T.K. Ahn, T.J. Avenson, M. Ballottari, Y.C. Cheng, K.K. Niyogi, R. Bassi, G.R. Fleming, Architecture of a charge-transfer state regulating light harvesting in a plant antenna protein, Science 320 (2008) 794–797.
[10] Y. Miloslavina, A. Wehner, P.H. Lambrev, E. Wientjes, M. Reus, G. Garab, R. Croce, A.R. Holzwarth, Far-red fluorescence: a direct spectroscopic marker for LHCII oligomer formation in non-photochemical quenching, FEBS Lett. 582 (2008) 3625–3631.
[11] R. Berera, C. Herrero, I.H.M. van Stokkum, M. Vengris, G. Kodis, R.E. Palacios, H. van Amerongen, R. van Grondelle, D. Gust, T.A. Moore, A.L. Moore, J.T.M. Kennis, A simple artificial light-harvesting dyad as a model for excess energy dissipation in oxygenic photosynthesis, Proc. Natl. Acad. Sci. U. S. A. 103 (2006) 5343–5348.
[12] A.V. Ruban, R. Berera, C. Ilioaia, I.H.M. van Stokkum, J.T.M. Kennis, A.A. Pascal, H. van Amerongen, B. Robert, P. Horton, R. van Grondelle, Identification of a mechanism of photoprotective energy dissipation in higher plants, Nature 450 (2007) 575–579.
[13] A.A. Pascal, Z.F. Liu, K. Broess, B. van Oort, H. van Amerongen, C. Wang, P. Horton, B. Robert, W.R. Chang, A. Ruban, Molecular basis of photoprotection and control of photosynthetic light-harvesting, Nature 436 (2005) 134–137.
[14] S. Bode, C.C. Quentmeier, P.N. Liao, N. Hafi, T. Barros, L. Wilk, F. Bittner, P.J. Walla, On the regulation of photosynthesis by excitonic interactions between carotenoids and chlorophylls, Proc. Natl. Acad. Sci. U. S. A. 106 (2009) 12311–12316.
[15] A.V. Ruban, P. Horton, Mechanism of delta-Ph-dependent dissipation of absorbed excitation-energy by photosynthetic membranes. 1. Spectroscopic analysis of isolated light-harvesting complexes, Biochim. Biophys. Acta 1102 (1992) 30–38.
[16] C. Ilioaia, M.P. Johnson, P. Horton, A.V. Ruban, Induction of efficient energy dissipation in the isolated light-harvesting complex of photosystem II in the absence of protein aggregation, J. Biol. Chem. 283 (2008) 29505–29512.
[17] T.P.J. Kruger, V.I. Novoderezhkin, C. Ilioaia, R. van Grondelle, Fluorescence spectral dynamics of single LHCII trimers, Biophys. J. 98 (2010) 3093–3101.
[18] R. Standfuss, A.C.T. van Scheltinga, M. Lamborghini, W. Kuhlbrandt, Mechanisms of photoprotection and nonphotochemical quenching in pea light-harvesting complex at 2.5A resolution, EMBO J. 24 (2005) 919–928.
[19] Z.F. Liu, H.C. Yan, K.B. Wang, T.Y. Kuang, J.P. Zhang, L.L. Gui, X.M. An, W.R. Chang, Crystal structure of spinach major light-harvesting complex at 2.72 angstrom resolution, Nature 428 (2004) 287–292.
[20] T. Barros, A. Royant, J. Standfuss, A. Dreuw, W. Kuhlbrandt, Crystal structure of plant light-harvesting complex shows the active, energy-transmitting state, EMBO J. 28 (2009) 298–306.
[21] B. van Oort, A. Marechal, A.V. Ruban, B. Robert, A.A. Pascal, N.C.A. de Ruijter, R. van Grondelle, H. van Amerongen, Different crystal morphologies lead to slightly different conformations of light-harvesting complex II as monitored by variations of the intrinsic fluorescence lifetime, Phys. Chem. Chem. Phys. 13 (2011) 12614–12622.
[22] A. Pandit, N. Shirzad-Wasei, L.M. Wlodarczyk, H. van Roon, E.J. Boekema, J.P. Dekker, W.J. de Grip, Assembly of the major light-harvesting complex II in lipid nanodiscs, Biophys. J. 101 (2011) 2507–2515.
[23] A. Pandit, H.J.M. de Groot, Solid-state NMR applied to photosynthetic light-harvesting complexes, Photosynth. Res. 111 (2012) 219–226.
[24] A. Pandit, F. Buda, A.J. van Gammeren, S. Ganapathy, H.J.M. de Groot, Selective chemical shift assignment of bacteriochlorophyll a in uniformly [(13)C–(15)N]-labeled light-harvesting 1 complexes by solid-state NMR in ultrahigh magnetic field, J. Phys. Chem. B 114 (2010) 6207–6215.
[25] A. Pandit, P.K. Wawrzyniak, A.J. van Gammeren, F. Buda, S. Ganapathy, H.J.M. de Groot, Nuclear magnetic resonance secondary shifts of a light-harvesting 2 complex reveal local backbone perturbations induced by its higher-order interactions, Biochemistry 49 (2010) 478–486.
[26] A. Pandit, T. Morosinotto, M. Reus, A.R. Holzwarth, R. Bassi, H.J.M. de Groot, First solid-state NMR analysis of uniformly (13)C-enriched major light-harvesting complexes from *Chlamydomonas reinhardtii* and identification of protein and cofactor spin clusters, Biochim. Biophys. Acta Bioenerg. 1807 (2011) 437–443.
[27] K. Arnold, L. Bordoli, J. Kopp, T. Schwede, The SWISS-MODEL workspace: a web-based environment for protein structure homology modelling, Bioinformatics 22 (2006) 195–201.
[28] F. Kiefer, K. Arnold, M. Kunzli, L. Bordoli, T. Schwede, The SWISS-MODEL repository and associated resources, Nucleic Acids Res. 37 (2009) D387–D392.
[29] T. Schwede, J. Kopp, N. Guex, M.C. Peitsch, SWISS-MODEL: an automated protein homology-modeling server, Nucleic Acids Res. 31 (2003) 3381–3385.
[30] N. Guex, M.C. Peitsch, SWISS-MODEL and the Swiss-PdbViewer: an environment for comparative protein modeling, Electrophoresis 18 (1997) 2714–2723.
[31] M.C. Peitsch, Protein modeling by e-mail, Biotechnology 13 (1995) 658–660.
[32] B. Han, Y.F. Liu, S.W. Ginzinger, D.S. Wishart, SHIFTX2: significantly improved protein chemical shift prediction, J. Biomol. NMR 50 (2011) 43–57.
[33] S. Gradmann, C. Ader, I. Heinrich, D. Nand, M. Dittmann, A. Cukkemane, M. van Dijk, A.M.J.J. Bonvin, M. Engelhard, M. Baldus, Rapid Prediction of multidimensional NMR data sets, J. Biomol. NMR 54 (2012) 377–387.
[34] B. van Oort, A. van Hoek, A.V. Ruban, H. van Amerongen, Aggregation of Light-Harvesting Complex II leads to formation of efficient excitation energy traps in monomeric and trimeric complexes, FEBS Lett. 581 (2007) 3528–3532.
[35] M.P. Johnson, A. Zia, P. Horton, A.V. Ruban, Effect of xanthophyll composition on the chlorophyll excited state lifetime in plant leaves and isolated LHCII, Chem. Phys. 373 (2010) 23–32.
[36] I. Moya, M. Silvestri, O. Vallon, G. Cinque, R. Bassi, Time-resolved fluorescence analysis of the photosystem II antenna proteins in detergent micelles and liposomes, Biochemistry 40 (2001) 12552–12561.
[37] R.J. Abraham, A.E. Rowan, Nuclear Magnetic Resonance Spectroscopy of Chlorophyll, in: H. Scheer (Ed.), Chlorophylls, CRC Press, 1991, pp. 797–834.
[38] V.I. Novoderezhkin, M.A. Palacios, H. van Amerongen, R. van Grondelle, Excitation dynamics in the LHCII complex of higher plants: modeling based on the 2.72 angstrom crystal structure, J. Phys. Chem. B 109 (2005) 10493–10504.
[39] M. Kloz, S. Pillai, G. Kodis, D. Gust, T.A. Moore, A.L. Moore, R. van Grondelle, J.T.M. Kennis, Carotenoid photoprotection in artificial photosynthetic antennas, J. Am. Chem. Soc. 133 (2011) 7007–7015.
[40] E. Wientjes, G. Roest, R. Croce, From red to blue to far-red in Lhca4: how does the protein modulate the spectral properties of the pigments? Biochim. Biophys. Acta Bioenerg. 1817 (2012) 711–717.
[41] C.D.P. Duffy, M.P. Johnson, M. Macernis, L. Valkunas, W. Barford, A.V. Ruban, A theoretical investigation of the photophysical consequences of major plant light-harvesting complex aggregation within the photosynthetic membrane, J. Phys. Chem. B 114 (2010) 15244–15253.
[42] X.P. Li, A.M. Gilmore, S. Caffarri, R. Bassi, T. Golan, D. Kramer, K.K. Niyogi, Regulation of photosynthetic light harvesting involves intrathylakoid lumen pH sensing by the PsbS protein, J. Biol. Chem. 279 (2004) 22866–22874.
[43] P.N. Liao, S. Pillai, M. Kloz, D. Gust, A.L. Moore, T.A. Moore, J.T.M. Kennis, R. van Grondelle, P.J. Walla, On the role of excitonic interactions in carotenoid-phthalocyanine dyads and implications for photosynthetic regulation, Photosynth. Res. 111 (2012) 237–243.
[44] G. Zucchelli, D. Brogioli, A.P. Casazza, F.M. Garlaschi, R.C. Jennings, Chlorophyll ring deformation modulates Q(y) electronic energy in chlorophyll-protein complexes and generates spectral forms, Biophys. J. 93 (2007) 2240–2254.
[45] F. Muh, M.E.A. Madjet, T. Renger, Structure-based identification of energy sinks in plant light-harvesting complex II, J. Phys. Chem. B 114 (2010) 13517–13535.
[46] L. Dall'Osto, S. Cazzaniga, H. North, A. Marion-Poll, R. Bassi, The *Arabidopsis* aba4-1 mutant reveals a specific function for neoxanthin in protection against photooxidative stress, Plant Cell 19 (2007) 1048–1064.
[47] T. Barros, W. Kuhlbrandt, Crystallisation, structure and function of plant light-harvesting complex II, Biochim. Biophys. Acta Bioenerg. 1787 (2009) 753–772.